MITSUBISHI ELECTRIC RESEARCH LABORATORIES
http://www.merl.com

Comparing Realtime Energy-Optimizing Controllers for Heat Pumps

Burns, Daniel J.; Bortoff, Scott A.; Laughman, Christopher R.; Guay, Martin

TR2018-100 July 13, 2018

Abstract

Two alternative realtime gradient descent algorithms for energy-optimizing control of a multi-zone heat pump system are considered. In the first approach, a model of the compressor and outdoor fan power consumption is used to obtain the gradient of power with respect to high- and low-side pressures and actuator settings. From this relationship, a gradient descent controller is obtained to drive the outdoor fan speed to a value that is predicted to minimize the power consumption. In the second approach, a time-varying extremum seeking controller is derived. Extremum seeking controllers estimate the gradient of the mapping between the system input and a measurement, and steers the input to a value that minimizes the measurement. Determination of the gradient information is model-free so that estimation and control are simultaneously performed on the system. As with the prior approach, the outdoor fan is controlled to a value that minimizes power. A multi-physical model of the heat pump is used to compare the controllers performance. The convergence rate is compared from an initial condition response where the outdoor fan is initialized to a suboptimal starting speed. The sensitivity to modeling error is judged by considering operating points distinct from the conditions at which linearization in the model-based approach is calculated. We show that because the model-based optimizer benefits from problem-specific information, convergence to a final value is faster than extremum seeking and that this final value is near the true optimizer, but not guaranteed to reach the true optimum in the presence of modeling errors. Conversely, we show that the extremum seeking converges more slowly that the model-based approach, but because ESC actively experiments with the plant online, the true optimizer is reached.

International Refrigeration and Air conditioning Conference at Purdue

Comparing Realtime Energy-Optimizing Controllers for Heat Pumps

Daniel J. Burns[1*] Scott A. Bortoff[1] Christopher R. Laughman[1] Martin Guay[2]

[1]Mitsubishi Electric Research Laboratories
Cambridge, MA, USA
burns@merl.com, bortoff@merl.com, laughman@merl.com
*corresponding author

[2]Queen's University
Department of Chemical Engineering
Kingston, Ontario
martin.guay@chee.queensu.ca

ABSTRACT

Two alternative realtime gradient descent algorithms for energy-optimizing control of a multi-zone heat pump system are considered. In the first approach, a model of the compressor and outdoor fan power consumption is used to obtain the gradient of power with respect to high- and low-side pressures and actuator settings. From this relationship, a gradient descent controller is obtained to drive the outdoor fan speed to a value that is predicted to minimize the power consumption.

In the second approach, a time-varying extremum seeking controller is derived. Extremum seeking controllers estimate the gradient of the mapping between the system input and a measurement, and steers the input to a value that minimizes the measurement. Determination of the gradient information is model-free so that estimation and control are simultaneously performed on the system. As with the prior approach, the outdoor fan is controlled to a value that minimizes power.

A multi-physical model of the heat pump is used to compare the controllers' performance. The convergence rate is compared from an initial condition response where the outdoor fan is initialized to a suboptimal starting speed. The sensitivity to modeling error is judged by considering operating points distinct from the conditions at which linearization in the model-based approach is calculated. We show that because the model-based optimizer benefits from problem-specific information, convergence to a final value is faster than extremum seeking and that this final value is near the true optimizer, but not guaranteed to reach the true optimum in the presence of modeling errors. Conversely, we show that the extremum seeking converges more slowly that the model-based approach, but because ESC actively experiments with the plant online, the true optimizer is reached.

1 INTRODUCTION

As actuators for vapor compression systems become increasingly electrified, commoditized and integrated with embedded systems, the controllability of the system is improved. For example, inverter-driven compressors, electronically-positioned expansion valves, and variable speed fans provide increased ability to regulate zone temperatures, reject heat load disturbances, and enforce constraints. When coupled with inexpensive temperature sensing and powerful embedded processors, the increase in flexibility has lead manufacturers to experiment with more sophisticated cycle configurations. Multi-zone air conditioners and heat pumps are now common: from a single outdoor heat exchanger and compressor, variable refrigerant flow machines modulate fluid pressure and flow rates to multiple indoor units to control their associated zone temperatures (Zhang *et al.*, 2017). And when a branch box is used to select either high or low pressure refrigerant to direct to the indoor units, a single outdoor unit may simultaneously provide both heating and cooling to the indoor zones.

As the vapor compression machine has become more sophisticated, the opportunities to improve efficiency are increasingly realized through the low-level control algorithms that coordinate machine actuators. However, designing controllers for this system is not straightforward: the heat load disturbances to be rejected are not measured, the governing dynamics are nonlinear and interactive, and the machine exhibits strong coupling between the multivariate inputs and outputs (Bonilla *et al.*, 2012). Further, the requirement to operate indoor unit heat exchangers as either condensers or evaporators force compromises in sensor locations and actuator selection. Despite these challenges, multivariable feedback controllers have been shown to effectively regulate zone temperatures to setpoints while enforcing constraints on actuator limits and key outputs (Burns *et al.*, 2018). However, there remains additional actuation authority that may be used to minimize steady state power consumption.

This paper considers the problem of controlling the outdoor fan speed of a multi-zone heat pump in order to minimize power consumption. We assume the vapor compression system is controlled by a preexisting feedback system that commands compressor speed and expansion valve positions in order to regulate zone temperatures. We further assume that an additional degree-of-freedom—the outdoor fan speed—is available to minimize power consumption in steady state.

In this context, two energy-optimizing controllers for the outdoor fan speed are derived and compared. The first method presented is model-based. Power consumption of the machine is assumed to be dominated by the compressor and outdoor fan, and the dependency of power on these actuators and the system state is modeled using standard polynomial relationships wherein coefficients are determined empirically. The gradient of this relationship with respect to actuator values and system pressures is computed and used to derive a gradient descent control law that drives the outdoor fan such that the system power consumption is minimized.

The second approach is model-free and based on the time-varying extremum seeking control algorithm. Briefly, extremum seeking controllers obtain an estimate of the gradient between a plant's manipulated inputs and an objective signal (i.e., power consumption) in order to steer the system toward an optimum operating point, under the assumption that this relationship is convex. Whereas traditional ESC methods exhibit slow and non-robust convergence, TV-ESC has demonstrated faster convergence due to the estimation routine that efficiently tracks the gradient as a time-varying parameter (Guay and Burns, 2017). This approach for extremum seeking has previously been applied to realtime optimization of vapor compression systems with faster convergence rates than traditional methods (Burns *et al.*, 2016, Weiss *et al.*, 2014)

The rest of the paper is organized as follows. Section 2 describes the system under consideration, the nominal feedback controller, and the control objectives. The model-based optimizer is derived in Section 3, and the time-varying extremum seeking controller is developed in Section 4. The performance of these two controllers is discussed in Section 5 using a physics-based model of a multi-zone heat pump. Finally, concluding remarks are offered in Section 6.

2 PROBLEM DESCRIPTION

This section briefly describes the operation of a multi-zone vapor compression system (VCS) and control inputs, measurements and objectives. The specific application considered in this paper employs the VCS as a heat pump, and therefore certain assumptions on heat exchanger type, refrigerant flow direction and control objectives have been made, although other applications of VCS (refrigeration, air conditioning, etc.) can be considered with straightforward substitutions of machine configurations.

2.1 Physical Description

The arrangement of the principal components of the multi-zone VCS are shown in Fig. 1A. Low pressure refrigerant in the vapor state enters the compressor suction port. The compressor performs work on the refrigerant to increase the pressure and temperature, and the amount of work is controlled by the compressor rotational frequency CF. A sensor measures the refrigerant discharge temperature Td exiting the compressor. High temperature and pressure

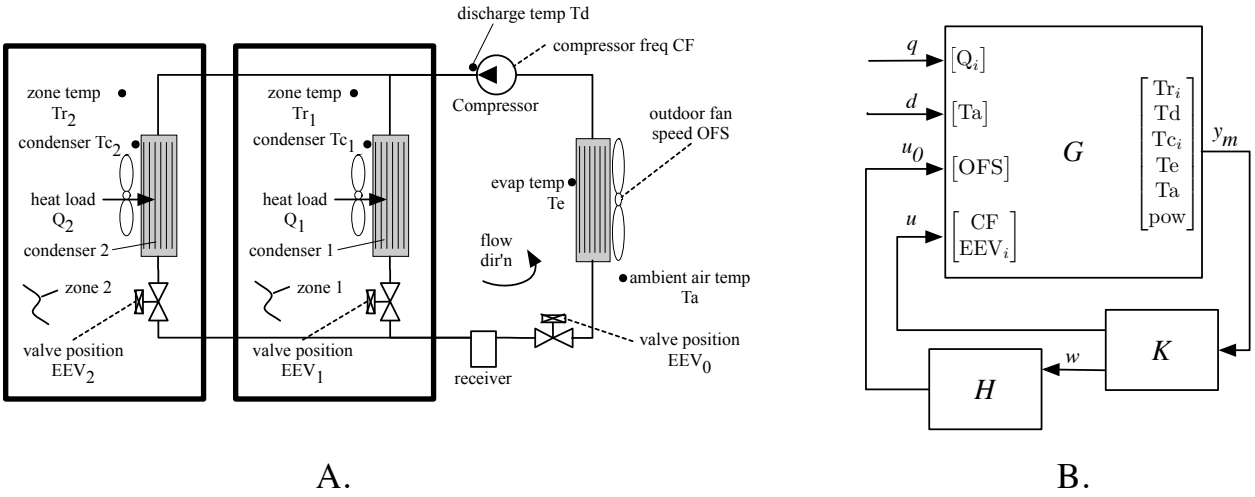

Figure 1: (A) Piping diagram of the multi-zone vapor compression system operating in heating mode. (B) The heat pump and zone dynamics G are controlled by feedback controller K that regulates zone temperatures and properties of the refrigerant cycle using the compressor frequency and expansion valves. The outdoor fan is controlled by a realtime optimizer H designed to minimized power.

refrigerant is then routed to multiple indoor heat exchangers across which a fan forces air. Heat is removed from the refrigerant and rejected to the air in the zones, which are at temperatures measured by zone sensors $\mathrm{Tr_i}, i = 1, \ldots, N$, where N is the number of zones. As the specific enthalpy of the refrigerant is reduced inside the heat exchangers, it condenses and ultimately exits as a high pressure liquid. The refrigerant then flows through through a set of electronic expansion valves which simultaneously reduce the pressure and temperature in an isenthalpic process. The electronic expansion valve positions ($\mathrm{EEV}_i, i = 1, \ldots, N$) controls the size of the valve orifice. For the system considered, an additional collective expansion valve EEV_0 is an available degree-of-freedom for regulating overall cycle pressures and cumulative refrigerant flow rate. The low pressure, low temperature refrigerant exiting the valves is a two-phase mixture of liquid and vapor and is passed to another heat exchanger. A fan forces air across the heat exchanger. The outdoor fan speed OFS controls the volumetric flow rate of air across the heat exchanger. Heat is absorbed by the refrigerant from the ambient air, which is at a temperature measured by an ambient temperature sensor, T_a. The ambient temperature is considered a measured disturbance. As the specific enthalpy of the refrigerant increases, it evaporates and exits the heat exchanger as a low pressure vapor. The refrigerant is routed to the compressor inlet, completing the cycle. Finally, heat loads $\mathrm{Q}_i, i = 1, \ldots, N$ are assumed in the zones and are unmeasured disturbances. If the energy supplied by the local condenser balances the heat load, the zone temperature does not change, otherwise the zone temperature will increase or decrease when the energy added by the condenser is greater or less than the heat load.

2.2 Controller Architecture

The control objective is to regulate the zone temperatures Tr_i to setpoints determined by an occupant, rejecting disturbances from changes in heat load Q_i and ambient air temperature Ta. Further, power consumption p is to be minimized at steady state. A Weiner model G of the system operating around an equilibrium consists of linear dynamics and a memory-less (static) nonlinear output function

$$\dot{x} = Ax + Bu + B_0 u_0 + B_d d + B_q q \quad (1)$$
$$y = Cx + D_d d \quad (2)$$
$$z = Ex + Fu + F_0 u_0 + F_d d \quad (3)$$
$$p = h(z, u, u_0), \quad (4)$$

where x is the state, $u = [\mathrm{CF}\ \mathrm{EEV}_i]^T$ are the inputs controlled by the feedback controller, $u_0 = \mathrm{OFS}$ is the outdoor fan

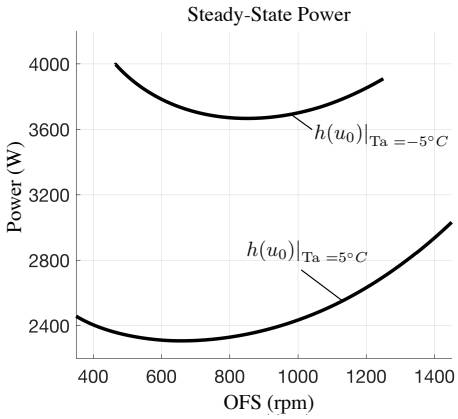

Figure 2: The steady-state power consumption h as a function of outdoor fan speed is shown for two fixed ambient air temperatures $\mathrm{Ta} = \{-5, 5\}°C$.

speed controlled by the power optimizing controller, d is the measured ambient air temperature disturbance, $q \in \mathfrak{R}^N$ are the unmeasured heat load disturbances, $y = [\mathrm{Tr}_i\ \mathrm{Td}\ \mathrm{Tc}_i\ \mathrm{Te}\ \mathrm{Ta}]^T$ is a vector of measured temperatures, $z = [\mathrm{p_S}\ \mathrm{p_D}]^T$ is a vector of suction and discharge pressures and p is the power consumption.

The control architecture is shown in Fig. 1B[1]. A multivariable feedback controller K is designed to drive the room temperature errors to zero. The feedback controller has access to $y_m = [y\ p]^T$ which consists of the temperature and power measurements. For a detailed description of K designed using H_∞ loop-shaping techniques, see Bortoff *et al.* (2018). This controller has an observer-based structure and is configured to output estimates $\hat{z}$ of z. For the present work, the suction and discharge pressures may be assumed available either from an estimator in K, or directly from temperature sensors Tc and Te and a temperature–pressure lookup table for the refrigerant employed. The inner-loop feedback system with G and K meets the regulation and disturbance rejection requirements. The power minimization is achieved in the outer-loop system consisting of G, K and H in feedback as shown in Fig. 1B.

The input to the optimization controller is labeled w and its definition depends on the optimization strategy. For the model-based optimizer considered in Section 3, this signal is the pressures, fan speed and compressor speed, $w = [z_1\ z_2\ u_0\ u_1]$. For the extremum seeking controller of Section 4, we define $w = p$, which we assume is measured. The optimization controller H receives the signal w from the feedback controller and directs the outdoor fan speed u_0 such that power p is minimized. The objective is to steer the control input u_0 to the optimizer of the steady state map $h(z, u, u_0^*)$. Note that due to the coupling inherent in the vapor compression system and the design of the feedback controller K, changing the outdoor fan speed will cause a change in all other actuators. Therefore, to minimize total machine power consumption it is sufficient to manipulate only the outdoor fan speed. Finally we note that for fixed u, d and q, the relationship between u_0 and h is convex and the equilibrium cost $h(u_0^*)$ satisfies the following optimality conditions:

$$\frac{\partial h(u_0^*)}{\partial u_0} = 0 \tag{5}$$

$$\frac{\partial^2 h(u_0^*)}{\partial u_0 \partial u_0^T} > \beta I \quad \forall u_0 \in U_0 \tag{6}$$

where β is a strictly positive constant and U_0 is the set of permissible outdoor fan speed inputs. This relationship is illustrated for two ambient temperatures in Fig. 2. In the following sections, two alternative power-optimizing controllers are considered for H. The next section describes a model-based optimizer.

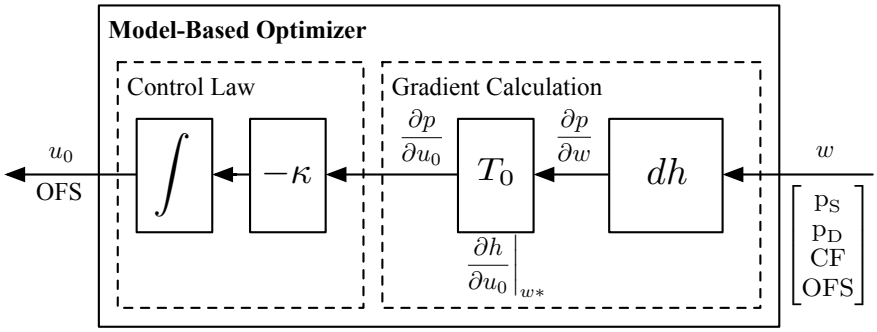

Figure 3: Power-minimizing feedback loop. The output of the dh block is $\frac{\partial p}{\partial w}$. By the chain rule, the output of the T_0 block is $\frac{\partial p}{\partial u_0}$ at steady-state. The gradient feedback forces $\dot{u}_0 = -\kappa \frac{\partial p}{\partial u_0}$. The feedback loop is exponentially stable for sufficiently small $\kappa > 0$.

3 MODEL-BASED OPTIMIZER

We begin by considering the SISO system with input u_0 and output p, and assume that (5)-(6) apply. The outdoor fan and compressor account for all of the modeled power consumption, so (4) can be written

$$p = h(z, u_0, u_1) = p_c(z_1, z_2, u_1) + p_f(u_0), \tag{7}$$

where the fan power p_f is modeled as a cubic polynomial in fan speed,

$$p_f(u_0) = \gamma_0 + \gamma_1 \cdot u_0 + \gamma_2 \cdot u_0^2 + \gamma_3 \cdot u_0^3. \tag{8}$$

Similarly, the compressor power p_c is modeled as

$$p_c(z_1, z_2, u_1) = \zeta_1(u_1) + \zeta_2(u_1) \cdot z_1 \cdot \eta_V \cdot u_1 \cdot V_{\text{disp}} \cdot \left(\frac{z_2}{z_1}\right)^{\zeta_3(u_1)} + \zeta_4(u_1) \cdot z_1 \cdot \eta_V \cdot u_1 \cdot V_{\text{disp}} \tag{9}$$

where the volumetric efficiency is

$$\eta_V(\omega, z_2, z_1) = \theta_1(u_1) + \theta_2(u_1) \cdot \left(\frac{z_2}{z_1}\right) + \theta_3(u_1) \cdot \left(\frac{z_2}{z_1}\right)^2 + \theta_4(\omega) \cdot (z_2 - z_1) + \theta_5(\omega) \cdot z_1 \cdot (z_2 - z_1). \tag{10}$$

ω is the compressor rotational speed, V_{disp} is the compressor displacement, and $\theta_j(u_1) = \beta_{j0} + \beta_{j1} u_1$, $\zeta_i(u_1) = \alpha_{i0} + \alpha_{i1} u_1 + \alpha_{i2} u_1^2$ for $i = 1, \ldots, 4$ and $j = 1, \ldots, 5$ (Threlkeld, 1970). The parameters γ_k, α_{ik} and β_{jk} are tuned empirically. Models such as (8)-(10) are often used by manufacturers for system design and can be known accurately.

Define $w = [z_1\ z_2\ u_0\ u_1]^T$ and let $T(s)$ denote the 4×1 closed-loop transfer function (with the inner loop GK closed) from u_0 to w. Also, define the steady-state gain $T_0 = T(0)$. Then the power minimizing feedback is a gradient descent controller

$$u_0(t) = -\kappa \int_0^t dh\,(w(\tau)) \cdot T_0\, d\tau \tag{11}$$

for $\kappa > 0$, where the gradient

$$dh = \frac{\partial h}{\partial w}$$

is computed symbolically from (7)-(10). A block diagram of this model-based optimizer is shown in Fig. 3. The closed loop system with is locally exponentially stable for sufficiently small $\kappa > 0$. For a proof of this claim, see the details in Bortoff *et al.* (2018).

[1] All control algorithms discussed in this paper are developmental and are not representative of any manufacturer's production controller.

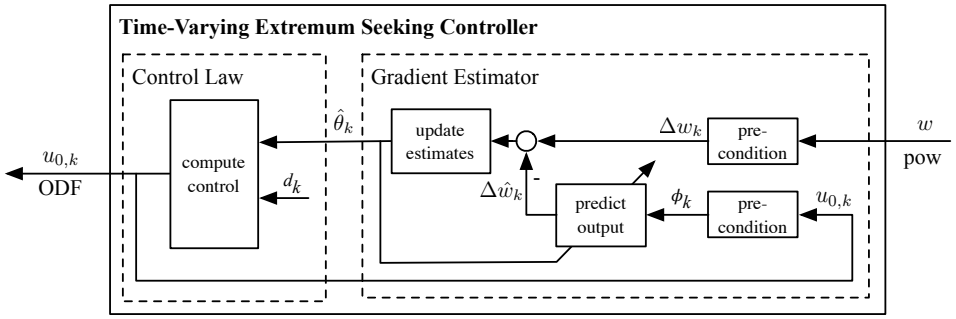

Figure 4: Time-varying extremum seeking controller block diagram.

In effect (11) drives u_0 to a condition in which dh is orthogonal to T_0, at which point the power is at a local minimum. Note that although the estimated power is used in the feedback, there is no need to invoke a timescale separation (as is common in extremum seeking) because the dynamics of the estimate error do not depend on u_0, and the closed-loop dynamics from G in feedback with K are explicitly incorporated into T. The gain κ must be limited because T may contain right half plane zeros in general, so sufficiently high gain may result in instability. This result is local because dh has higher-order terms that effectively increase the feedback gain for large values of initial conditions, although we do not find this to be a problem in practice. Finally, we do not find the "slowly-varying" assumption to be practically limiting. In practice the closed-loop system is stable for step changes in references and disturbances, as demonstrated in Section 5.

4 EXTREMUM SEEKING CONTROLLER

As with the model-based optimizer, the extremum seeking controller (ESC) is configured to drive the ODF u_0 such the the overall power consumption is minimized. In contrast to the MBO, note that the ESC only requires a measurement of the power consumption, and with abuse of notation we redefine w in this section to consist only of a measurement of the power $w = p$. Referring to Fig. 1B, note that any or all of the measurements provided to the feedback controller K may be passed directly to the optimizer H, including the measurement of power. To derive the discrete-time extremum seeking controller, we follow the derivation outlined in Guay (2014).

Let $\phi_k = \Delta u_{0,k}$. The dynamics of the cost function can be parametrized as:

$$\Delta w_k = \theta_k^T \Delta u_{0,k} = \phi_k^T \theta_k. \tag{12}$$

Let the estimator for (12) be

$$\Delta \hat{w}_k = \hat{\theta}_k^T \Delta u_{0,k} = \phi_k^T \hat{\theta}_k \tag{13}$$

where $\hat{\theta}_k$ is the vector of parameter estimates and is a local estimate of the gradient. As the system is driven toward the optimizer, clearly this estimated gradient will change over time, and the estimation routine is informed by time-varying parameter estimators. Consequently this algorithm is termed time-varying extremum seeking control (TV-ESC). The output prediction error is defined as $e_k = \Delta w_k - \Delta \hat{w}_k$. The dynamical system operates at the faster time-scale with sampling time $\epsilon \Delta t$ while the steady-state optimization operates at the slow time scale with sampling time Δt, where ϵ is a time-scale separation parameter. The parameter estimates are updated as follows:

$$\Sigma_{k+1}^{-1} = \Sigma_k^{-1} + \epsilon \left(\frac{1}{\alpha} - 1 \right) \Sigma_k^{-1} - \frac{\epsilon}{\alpha^2} \Sigma_k^{-1} \phi_k (1 + \frac{1}{\alpha} \phi_k^T \Sigma_k^{-1} \phi_k)^{-1} \phi_k^T \Sigma_k^{-1} \tag{14}$$

$$\bar{\hat{\theta}}_{k+1} = \text{Proj} \left[\hat{\theta}_k + \frac{\epsilon}{\alpha} \Sigma_k^{-1} \phi_k (1 + \frac{1}{\alpha} \phi_k^T \Sigma_k^{-1} \phi_k)^{-1} (e_k), \Theta_0 \right] \ . \tag{15}$$

Where $\Sigma \in \mathbb{R}^{n_\theta \times n_\theta}$ is the covariance matrix and Proj is an orthogonal projection operator. For a more detailed discussion on this operator see Goodwin and Sin (2013).

The gradient descent controller is given by:

$$u_{0,k+1} = u_{0,k} - \epsilon k_g \hat{\theta}_k + \epsilon d_k \tag{16}$$

where d_k is a bounded dither signal and k_g is the optimization gain .

Together, the iterative extremum seeking routine is given by:

$$u_{0,k+1} = u_{0,k} - \epsilon k_g \hat{\theta}_k + \epsilon d_k \tag{17a}$$

$$\phi_k = \Delta u_{0,k} = u_{0,k+1} - u_{0,k} \tag{17b}$$

$$\Delta \hat{w}_k = \phi_k^T \hat{\theta}_k \tag{17c}$$

$$\Sigma_{k+1}^{-1} = \Sigma_k^{-1} + \epsilon(\frac{1}{\alpha} - 1)\Sigma_k^{-1} - \frac{\epsilon}{\alpha^2}\Sigma_k^{-1}\phi_k(1 + \frac{1}{\alpha}\phi_k^T\Sigma_k^{-1}\phi_k)^{-1}\phi_k^T\Sigma_k^{-1} \tag{17d}$$

$$\bar{\hat{\theta}}_{k+1} = Proj\left[\hat{\theta}_k + \frac{\epsilon}{\alpha}\Sigma_k^{-1}\phi_k(1 + \frac{1}{\alpha}\phi_k^T\Sigma_k^{-1}\phi_k)^{-1}(e_k), \Theta_0\right] \quad . \tag{17e}$$

As shown in Figure 4, at the k^{th} iteration step, the ESC algorithm uses the difference between current $u_{0,k}$ and next outdoor fan input $u_{0,k+1}$, and the difference between measured Δz_k and predicted $\Delta \hat{z}_k$ change in power consumption for the gradient estimation. The estimated gradient is used to parameterize the unknown but measured cost function describing power consumption. The gradient is estimated by employing a recursive least squares filter with forgetting factor α. Further, the estimated gradient is used to compute the gradient descent controller which drives the outdoor fan speed such that power consumption is minimized.

Note that the time-varying extremum seeking controller does not require averaging the effect of the perturbation as in the case of a conventional perturbation-based extremum seeking controller. For this reason, time-varying extremum seeking converges faster than traditional methods (Burns *et al.*, 2016), although not as fast as the model-based approach as demonstrated in the next section.

5 RESULTS AND DISCUSSION

This section compares the performance of the two realtime optimization strategies using a multi-physical model of the multi-zone heat pump. A brief description of the physics-based model is provided, followed by simulation results and discussion.

5.1 Multi-physical Model Description

The physical system described in Section 2 and shown in Fig. 1A is modeled in the Modelica language (Modelica Association, 2017). Heat exchanger models are dynamic and discretized with finite volume approximations (1-D refrigerant side, 3-D air side). Similarly, the pipes connecting components and the receiver are dynamic models and capture pressure losses and refrigerant charge migration. The compressor model (partially described in Equations (9)–(10)) is algebraic and includes isentropic and volumetric efficiency relations that have been calibrated to experimental data. The valve models are also algebraic and assume isentropic expansion. The zones are modeled as lumped-air volumes with heat transfer through convective boundary conditions and an insulated envelope to the ambient environment. The air is modeled as an ideal gas description of dry air. The refrigerant model uses the full technical equations of state, and pressure and specific enthalpy are used as the state variables for the refrigerant in each pipe volume. The heat transfer coefficients and frictional pressure losses are based on simplified empirical correlations, and have been calibrated to data obtained in an calorimetric-style HVAC laboratory. More information on this general modeling approach can be found in Laughman *et al.* (2015), and further details on the specific multi-zone heat pump model can be found in Qiao *et al.* (2017).

Additionally, the feedback controller K and the optimization controllers H are realized in Modelica. The model-based

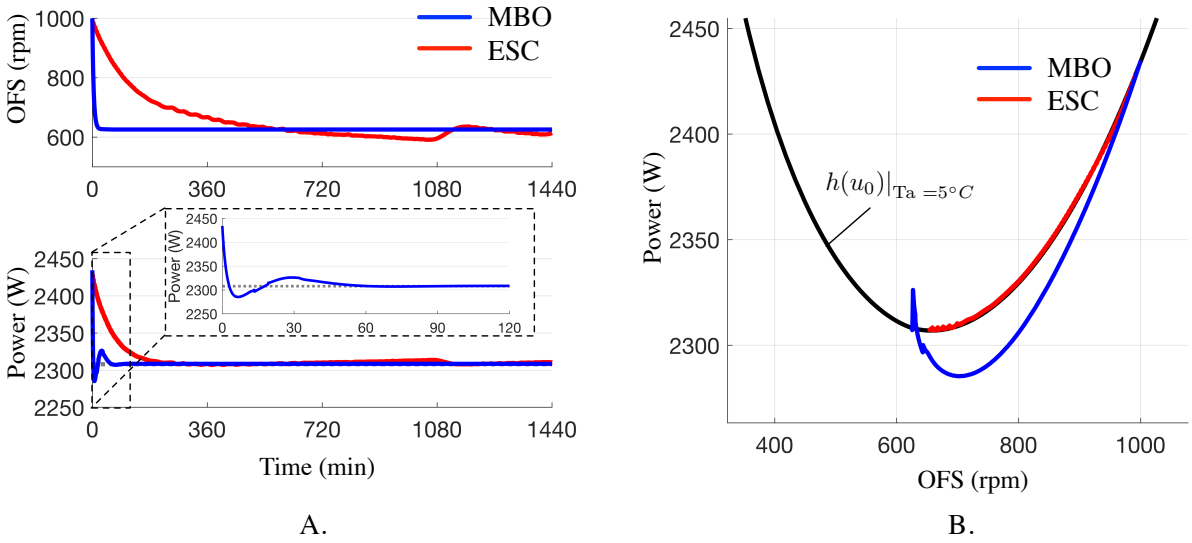

Figure 5: Comparison of realtime optimization controllers to a suboptimal initial condition with the ambient air temperature at Ta = 5°C. The model-based optimizer (MBO) is shown in blue and the extremum seeking controller (ESC) is shown in red. (A) The response of the control input and resulting power consumption as a function of time. (B) The responses overlaid on the steady state map for these conditions.

optimizer is continuous-time and implemented as a replaceable model, leveraging the object-oriented paradigm. Algebraic loops originating from a controller that simultaneously receives an outdoor fan speed (to compute the gradient of power) and determines the outdoor fan speed is transparently handled by Modelica's symbolic equation manipulations. The extremum seeking controller is discrete-time and the modeling framework uses a synchronous sampling routine to execute discrete-time components at fixed intervals.

The specific instance of the plant simulated below includes four zones ($N = 4$), the heat loads Q_i are set to approximately 50% of the full rated capacity for the indoor unit heat exchangers, and the ambient air temperature is selected from the set $\mathrm{Ta} = \{-5, 5\}°C$, depending on the simulation objective as described below. The feedback controller K is configured to regulate the zone temperatures to $\mathrm{Tr}_i = 27°C$. At these fixed conditions, each simulation is run for a extended time until initialization transients have settled. Results presented below begin after the startup transient has decayed. Two simulation studies are performed: the first compares the response of the two realtime optimization controllers to a scenario where the outdoor fan is initialized to a suboptimal speed, and the second considers the resulting disturbance rejection performance when a step change in ambient air temperature is applied.

5.2 Simulation Results

Fig. 5A shows the time-domain response of the outdoor fan speed (top) and resulting power consumption (bottom) when the fan is initialized to 1,000 rpm, Ta = 5°C, which results in $p = 2,427$ W. The true optimizer in this case is at $u_0^* = 613$ rpm and results in $p^* = 2,308$ W. At $t = 0$, both realtime optimization controllers are engaged.

We note that the DC-gain of the closed loop system T_0 is computed for the MBO at Ta = 5°C, and therefore we expect no modeling error to manifest in the MBO at this conditions. The extremum seeking controller, being model-free, should converge to the true optimizer regardless of system perturbations, provided that Equations (5)-(6) are satisfied. Indeed, both realtime optimizers drive the system to the optimizer. However, while MBO converges within about 60 min (see inset plot), the ESC first reaches the optimum fan speed in about 600 min, and remains in a neighborhood subsequently. The convergence trajectory can be viewed in Fig. 5B, which plots power as a function of fan speed where time is implicit. The ESC trajectory closely follows the steady state map, indicating that system dynamics are

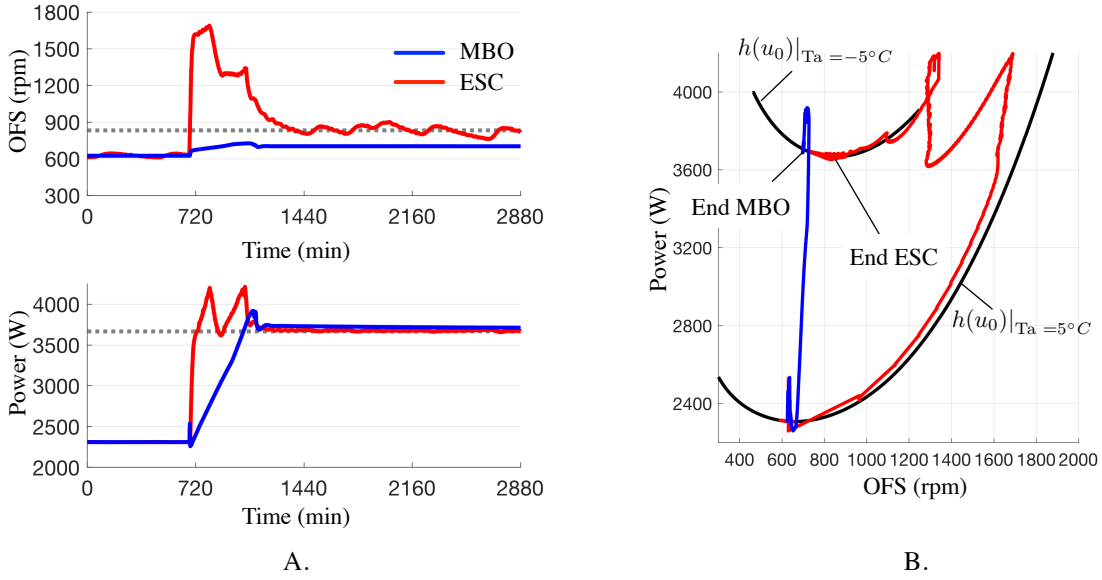

Figure 6: Comparison of realtime optimization controllers to step change in the outdoor air temperature.

not substantially excited. However, we expect time-varying extremum seeking to robustly estimate gradients while the system state is changing (indeed, this was the motivation for the development of this algorithm), and we attribute the slower than expected convergence of ESC in this instance to conservative tuning of the algorithm parameters. We note that one particular advantage of the MBO approach is the single tuning parameter κ has an intuitive relationship with convergence speed, whereas TV-ESC has several parameters that must be iteratively adjusted.

Fig. 6 shows the response of both methods to a step change in outdoor air temperature. Initially, the system is operated at Ta $= 5°C$, then at $t = 680$ min, the ambient air temperature is decreased to Ta $= -5°C$. The feedback controller K drives the compressor and expansion valves to regulate the zone temperatures despite the lower ambient conditions, and therefore the steady state power map is increased. At the same time, the realtime optimizers drive the outdoor fan such that the minimum power is obtained.

Both methods converge in approximately the same period (MBO in 520 min, ESC in 700 min). However, the MBO arrives at a fan speed 130 rpm below optimum of $u_0^* = 833$ rpm, whereas the ESC remains in a neighborhood ($u_{0,\mathrm{ESC}} = u_0^* \pm 40$ rpm) around the true optimum. The curvature of steady state map around the minimum is low, and therefore the resulting suboptimal power consumption for MBO is not significant (60 W suboptimal, or about 1.6%). Finally, we point out that fan speeds selected by the MBO during the transient has smaller amplitude compared to ESC, which overshoots to 1,700 rpm before the gradient estimate is appropriately updated. In fact, because the MBO's calculation of the outdoor fan speed depends explicitly on the VCS states, as long as the inner loop system GK is designed such that all closed loop poles are in the open left half plane, than the additional integrator contributed by the MBO will guarantee exponential stability for sufficiently small κ. Similar claims of stability for ESC are not generally available.

6 CONCLUSION

Two realtime optimization controllers for a multi-zone vapor compression system are considered. Both are shown to automatically drive the system to values that minimize power under assumptions of convexity, and (in the case of a model-based optimizer,) when the operating conditions are near the point at which the DC-gain is computed. The time-varying extremum seeking controller, while faster than traditional ESC approaches, does not reach the optimum at the same rate as the model-based optimizer, but always finds the true optimizer. Suboptimal results attained by

the MBO is attributed to two sources: (1) the DC-gain term T_0 computed at particular conditions will be incorrect at other points due to the nonlinear governing physics and (2) general modeling errors that manifest in calculations of the derivative *dh*. While the sensitivity to (1) is briefly discussed, contributions from (2) have not been addressed here and are planned for future work.

The two approaches exhibit various benefits and drawbacks that lend themselves to different applications: the guaranteed stability performance of MBO may be appropriate for realtime operation in unstructured environments where some suboptimality in power consumption can be tolerated, and the property of robust convergence to the true optimizer exhibited by TV-ESC may be suitable for (semi-)supervised situations such as factory calibration or in cases where obtaining a model is not feasible and optimal performance is required.

REFERENCES

Bonilla, J., Yebra, L.J., Dormido, S., and Cellier, F.E. Object-oriented library of switching moving boundary models for two-phase flow evaporators and condensers. In *Proceedings of the 9th International Modelica Conference*, pages 71–80 (2012).

Bortoff, S.A., Burns, D.J., Laughman, C.R., Qiao, H., Danielson, C., Goldsmith, A., and Di Cairano, S. Power Optimizing Control of Multi-Zone Heat Pumps. In *IEEE Conference on Control Technology and Applications* (2018).

Burns, D.J., Danielson, C., Zhou, J., and Di Cairano, S. Reconfigurable model predictive control for multi-evaporator vapor compression systems. *IEEE Transactions on Control Systems Technology*, 26(3):984–1000 (2018).

Burns, D.J., Laughman, C.R., and Guay, M. Proportional–integral extremum seeking for optimizing power of vapor compression systems. In *International Refrigeration and Air Conditioning Conference at Purdue* (2016).

Goodwin, G. and Sin, K. *Adaptive Filtering Prediction and Control*. Dover Books on Electrical Engineering Series. Dover Publications, Incorporated (2013). ISBN 9780486137728.

Guay, M. A time-varying extremum-seeking control approach for discrete-time systems. *Journal of Process Control*, 24(3):98 – 112 (2014).

Guay, M. and Burns, D.J. A proportional integral extremum-seeking control approach for discrete-time nonlinear systems. *International Journal of Control*, 90(8):1543–1554 (2017).

Laughman, C., Qiao, H., Aute, V., and Radermacher, R. A comparison of transient heat pump cycle models using alternative flow descriptions. *Science and Technology for the Built Environment*, 21(5):666–680 (2015).

Modelica Association. Modelica specification, Version 3.4 (2017).

Qiao, H., Laughman, C., Burns, D., and Bortoff, S. Dynamic characteristics of an R410A multi-split variable refrigerant flow air-conditioning system. In *12th IEA Heat Pump Conference* (2017).

Threlkeld, J. *Thermal Environmental Engineering*. Prentice Hall (1970).

Weiss, W.K., Burns, D.J., and Guay, M. Realtime optimization of mpc setpoints using time-varying extremum seeking control for vapor compression machines. In *International Refrigeration and Air Conditioning Conference at Purdue* (2014).

Zhang, X., Shi, W., Hu, Q., Yan, B., Malkawi, A., and Li, N. Distributed temperature control via geothermal heat pump systems in energy efficient buildings. In *2017 American Control Conference (ACC)*, pages 754–760 (2017). doi:10.23919/ACC.2017.7963043.